2024, **25** (3), 315–325. doi 10.26089/NumMet.v25r324

doi 10.26089/NumMet.v25r324

New land use parameterization for INM-CM terrestrial carbon cycle module

Alexey Yu. Chernenkov
Marchuk Institute of Numerical Mathematics RAS, Moscow, Russia
Institute of Geography RAS, Moscow, Russia
Moscow Institute of Physics and Technology (National Research University), Dolgoprudny, Russia
ORCID: 0000-0003-0195-7608, e-mail: chernenkoval97@gmail.com

Evgeny M. Volodin
Marchuk Institute of Numerical Mathematics RAS, Moscow, Russia
Institute of Geography RAS, Moscow, Russia
ORCID: 0000-0003-1073-7287, e-mail: volodinev@gmail.com

Abstract: This paper presents a new version of the terrestrial carbon cycle module for the INM RAS Earth system model family (INM-CM). Its main difference from the previous one is a more detailed account of anthropogenic impacts on land ecosystems. This article describes a new land use database for INM-CM that takes into account changes in the spatial distribution of vegetation from 1850 to 2100. Harvesting in cultivated areas is also accommodated in the new version of the model. Numerical simulations are performed with the original and modified versions of the terrestrial carbon cycle module, covering both the historical period (1850–2014) and the possible future scenario (2015–2100). Estimates of the change in global land carbon stocks compared to the end of the pre-industrial period are obtained. The paper also proposes an effective way to prepare the initial state of carbon pools using the terrestrial carbon cycle module in stand-alone mode.

Keywords: carbon cycle, land use, climate, Earth system modelling.

Acknowledgements: The authors are grateful to Alexey Viktorovich Eliseev for important discussions of the model equations, as well as to Maria Tarasevich and an anonymous reviewer for valuable comments on the presentation of the research results. The research was carried out at the Marchuk Institute of Numerical Mathematics of the Russian Academy of Sciences. The development of the new terrestrial carbon cycle module is supported by the Russian Science Foundation, project 20–17–00190. Performing of numerical simulations of land carbon storage is funded by the Russian Federation research and technical development program in ecological strategy and climate change through grant FFMG–2023–0001 "Development of an extended version of the INM RAS Earth system model within a new computational framework".

For citation: A. Yu. Chernenkov, E. M. Volodin, "New land use parameterization for INM-CM terrestrial carbon cycle module," Numerical Methods and Programming. **25** (3), 315–325 (2024). doi 10.26089/NumMet.v25r324.

2024, **25** (3), 315–325. doi 10.26089/NumMet.v25r324

Новая параметризация землепользования для модуля наземного углеродного цикла Модели Земной системы ИВМ РАН

А. Ю. Черненков
Институт вычислительной математики РАН имени Г. И. Марчука, Москва, Российская Федерация
Институт географии РАН, Москва, Российская Федерация
Московский физико-технический институт (национальный исследовательский университет), Долгопрудный, Российская Федерация
ORCID: 0000-0003-0195-7608, e-mail: chernenkoval97@gmail.com

Е. М. Володин
Институт вычислительной математики РАН имени Г. И. Марчука, Москва, Российская Федерация
Институт географии РАН, Москва, Российская Федерация
ORCID: 0000-0003-1073-7287, e-mail: volodinev@gmail.com

Аннотация: В данной работе представлена новая версия модуля углеродного цикла суши для семейства Моделей Земной системы ИВМ РАН. Ее основное отличие от предыдущей заключается в более подробном учете антропогенного влияния на наземные экосистемы. В статье описывается подготовка новой базы данных землепользования, иллюстрирующей изменения в пространственном распределении растительности с 1850 по 2100 годы. Кроме того, новая версия модели учитывает сбор урожая на возделываемых территориях. С исходной и модифицированной версиями модуля наземного углеродного цикла проведены вычислительные эксперименты, охватывающие как исторический период (1850–2014), так и возможный сценарий будущего (2015–2100). Получены оценки изменения глобальных запасов углерода суши по сравнению с концом прединдустриального периода. Также в работе предложен экономичный способ формирования начального состояния для углеродных пулов с помощью автономной версии модуля наземного углеродного цикла.

Ключевые слова: углеродный цикл, землепользование, климат, моделирование Земной системы.

Благодарности: Авторы выражают благодарность Алексею Викторовичу Елисееву за важные обсуждения уравнений модели, а также Марии Тарасевич и анонимному рецензенту за ценные замечания по изложению результатов исследования. Работа выполнена в Институте вычислительной математики имени Г. И. Марчука Российской академии наук. Разработка нового модуля наземного углеродного цикла поддержана Российским научным фондом (грант 20–17–00190). Проведение вычислительных экспериментов по моделированию запасов углерода на суше финансируется в рамках тематики “Создание расширенной версии модели Земной системы ИВМ РАН на базе новой вычислительной платформы” (грант FFMG–2023–0001) Федеральной научно-технической программы в области экологического развития Российской Федерации и климатических изменений.

Для цитирования: Черненков А.Ю., Володин Е.М. Новая параметризация землепользования для модуля наземного углеродного цикла Модели Земной системы ИВМ РАН // Вычислительные методы и программирование. 2024. **25**, № 3. 315–325. doi 10.26089/NumMet.v25r324.

1. Introduction. The concentration of greenhouse gases in the atmosphere, especially CO_2, plays a major role in modern climate change. Since 1850, the CO_2 content in the atmosphere has been increasing every year in response to anthropogenic emissions [1]. However, the uptake of carbon (C) from atmospheric CO_2 by land ecosystems and its dissolution in the oceans slows this rate [2]. Therefore, future projections of the absorption of anthropogenic carbon emissions have not only scientific but also practical relevance for humanity.

The efficiency of CO_2 uptake by the terrestrial ecosystems depends on their type and their spatial distribution. Since the second half of the 20th century, human land use activities have resulted in significant changes to

2024, **25** (3), 315–325. doi 10.26089/NumMet.v25r324

the Earth's surface and ecosystems, affecting climate both directly and through feedbacks on carbon uptake [3]. In the future, land use activities are likely to expand and intensify further to meet growing demands for food, fibre, and energy [4]. It is crucial to take these changes into account for accurate future projections of CO_2 uptake by terrestrial ecosystems.

Earth system models are the main tool for climate change research today. The carbon cycle module is an essential part of them, as it plays a key role in determining the atmospheric response to human emissions of CO_2. These models have a large number of uncertainties, such as the amount of land vegetation and how it changes over time, as well as the emissions of various greenhouse gases. To solve this problem, a prescribed time-dependent data set of land cover and emissions can be used. Within the Coupled Model Intercomparison Project Phase 6 (CMIP6) [5], a harmonized vegetation database [6] and emissions data are prepared. They describe both the historical period and a set of future possible scenarios.

Land carbon cycle modules give absolute values of vegetation and soil carbon pools with a large scatter [7]. This fact and the lack of global data on soil carbon stocks make it difficult to verify these modules. However, there are data based on observations that describe global changes in carbon storage on the Earth (separately for atmosphere, land, ocean), such as the Global Carbon Project (GCP) [2]. Comparison of model data with this or a similar dataset can be used to evaluate the quality of the global land carbon store simulation. Models participating in the CMIP6 [5] show good agreement with these observations and also with each other for simulated changes in carbon stocks [1, 7].

There is a family of Earth system models developed at the Marchuk Institute of Numerical Mathematics RAS, called INM-CM. This group of models is constantly evolving, and today it includes a set of coupled models with different spatial resolutions, as well as various special modules. Model INMCM6 [8] is the current base version of INM-CM. It is a coupled atmosphere and ocean general circulation model, supplemented by an aerosol block and a sea ice model. In addition, the atmosphere model includes a number of parameterizations such as heat and moisture transfer in the soil [9], terrestrial carbon cycle [10] and others. The spatial resolution of the INMCM6 atmosphere model is $2.0^\circ \times 1.5^\circ$ in longitude and latitude.

This paper proposes a new version of the INM-CM terrestrial carbon cycle module. The main update is a more detailed accounting of anthropogenic impacts on ecosystems. The preparation of a new land use database is briefly described, and the updated model equations are formulated. The results of numerical simulations with the original and modified versions of the terrestrial carbon cycle module are presented both in a stand-alone mode and as part of the INMCM6.

2. Model description.

2.1. Original version of INM-CM terrestrial carbon cycle module. The original version of the terrestrial carbon cycle module used in INMCM6 [8] is presented in [10]. INM-CM uses a mosaic approach to describe the Earth's surface. It is assumed that several types of land cover can exist within a cell. Their set is similar to the one presented in [12] and includes 13 possible plant functional types (PFTs) and two additional non-vegetated types (bare soil and open water):

1. tropical forest
2. broadleaf-deciduous trees
3. mixed forest
4. needleleaf-evergreen trees
5. needleleaf-deciduous trees
6. trees of savanna
7. groundcover only
8. broadleaf shrubs with perennial groundcover
9. broadleaf shrubs with bare soil
10. tundra (trees)
11. tundra (groundcover)
12. cultivated areas (trees)
13. cultivated areas (groundcover)
14. bare soil
15. open water

The spatial distribution of PFT is assumed to be constant over time. INM-CM uses a vegetation cover data based on [13]. The coverage of the dominant vegetation types is shown in Fig. 1. For clarity, all types are reduced to four major groups: forest trees, groundcover (labelled as grass in the legend), tundra and cultivated areas (crops in the legend). Shrub types are not dominant in any of the model cells and are therefore not shown in this figure.

Land carbon stocks [$\mathrm{kg\,C\,/\,m^2}$] are divided into three main pools: vegetation carbon (C_{VEG}), soil carbon (C_{SOIL}) and rapidly degradable soil carbon associated with human activities ($C^{\mathrm{fast}}_{\mathrm{SOIL}}$). Through natural and

2024, **25** (3), 315–325. doi 10.26089/NumMet.v25r324

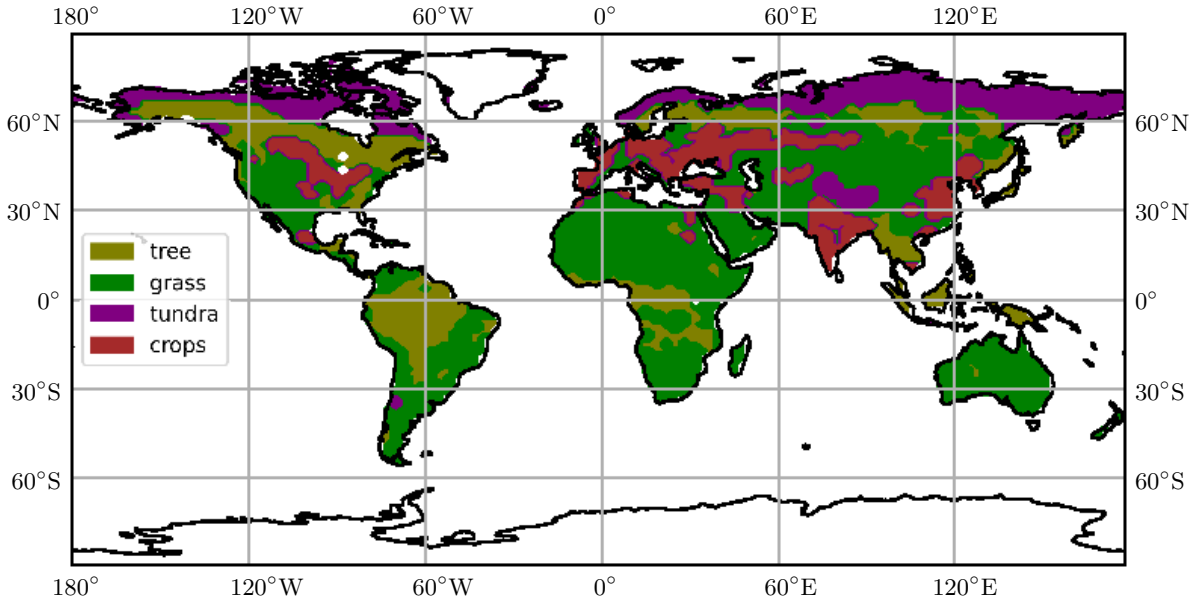

Figure 1. Original map of the dominant vegetation types used in INM-CM

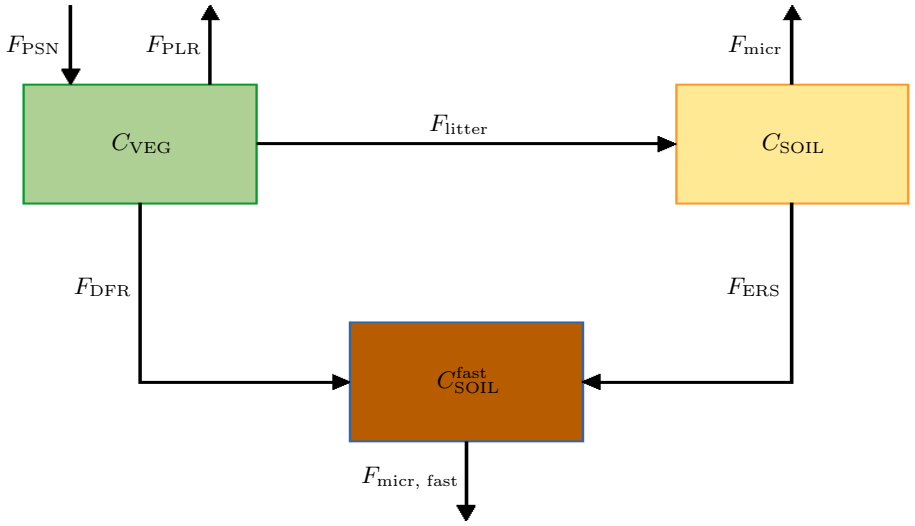

Figure 2. Conceptual scheme of INM-CM terrestrial carbon module

anthropogenic processes, carbon is captured by vegetation, moved into the soil and then released back into the atmosphere as CO_2 when it decomposes. The conceptual scheme of terrestrial carbon dynamics is illustrated in Fig. 2. It is described by the following balance equations, which are solved independently for each model land grid cell and separately for each of the 13 PFTs:

$$\frac{\partial C_{\mathrm{VEG}}}{\partial t} = F_{\mathrm{PSN}} - F_{\mathrm{PLR}} - \frac{C_{\mathrm{VEG}}}{\tau_{\mathrm{VEG}}} - F_{\mathrm{DFR}} \cdot C_{\mathrm{VEG}}, \tag{1}$$

$$\frac{\partial C_{\mathrm{SOIL}}}{\partial t} = \frac{C_{\mathrm{VEG}}}{\tau_{\mathrm{VEG}}} - \frac{C_{\mathrm{SOIL}}}{\tau_{\mathrm{SOIL}}} - F_{\mathrm{ERS}} \cdot C_{\mathrm{SOIL}}, \tag{2}$$

$$\frac{\partial C^{\mathrm{fast}}_{\mathrm{SOIL}}}{\partial t} = F_{\mathrm{DFR}} \cdot C_{\mathrm{VEG}} + F_{\mathrm{ERS}} \cdot C_{\mathrm{SOIL}} - \frac{C^{\mathrm{fast}}_{\mathrm{SOIL}}}{\tau_{\mathrm{fast}}}, \tag{3}$$

where F_{PSN} and F_{PLR} are the photosynthesis and plant respiration rates normalized to the PFT area in the model cell (calculated similarly to LSM-1.0 [11]). Land use effects are described by the time-independent intensity

2024, **25** (3), 315–325. doi 10.26089/NumMet.v25r324

Table 1. Characteristic turnover time of carbon pools, [years]

PFT	τ_{VEG}	τ_{SOIL}	τ_{fast}
tropical forest	8	5	0.1
broadleaf-deciduous trees	30	13	0.2
mixed forest	30	15	0.3
needleleaf-evergreen trees	30	45	0.6
needleleaf-deciduous trees	30	40	0.6
trees of savanna	20	20	0.4
groundcover only	1	20	0.4
broadleaf shrubs with perennial groundcover	30	17	0.3
broadleaf shrubs with bare soil	30	22	0.5
tundra (trees)	30	270	3.3
tundra (groundcover)	1	265	3.3
cultivated areas (trees)	30	30	0.6
cultivated areas (groundcover)	1	33	0.6

of deforestation F_{DFR} and soil erosion F_{ERS}. The values τ_{VEG}, τ_{SOIL} and τ_{fast} are PFT-specific characteristic times for plant death and soil decomposition (see Tab. 1), and the corresponding terms from the equations go with the fluxes F_{litter}, F_{micr} and $F_{\text{micr,fast}}$ on the scheme.

The numerical solution of equations (1)–(3) is obtained by the explicit Euler method. The time step is equal to one hour and is mainly determined by other modules of INM-CM describing land processes.

The total carbon stocks in a model land cell $\{C^k\}_{k=1}^{3} = \{C_{\text{VEG}}, C_{\text{SOIL}}, C_{\text{SOIL}}^{\text{fast}}\}$ are defined as the sum of all PFT sub-pools:

$$C^k = \sum_{j=1}^{13} C_j^k, \tag{4}$$

where $\{C_j^k\}_{j=1}^{13}$ is the set of solutions of system (1)–(3) for each PFT. Here, the quantity C_j^k characterizes the amount of stored carbon by the j PFT per unit area of the model cell.

2.2. New land cover database for INM-CM. A new land cover dataset for INM-CM is prepared using data from the Land Use Harmonization 2 (LUH2) project [6]. In contrast to the original permanent vegetation map used in INM-CM, the new database describes changes in PFTs spatial distribution from 1850 to 2100 with time step of one year.

Project LUH2 is a part of the CMIP6 [5], which aims to produce a consistent set of land use scenarios that linking historical reconstructions with future projections. The LUH2 database is a collection of spatial distributions of land cover types, as well as data on changes in land use types over time. Data are available for the period from 850 to 2300 with a spatial resolution of $0.25^\circ \times 0.25^\circ$. According to the LUH2 classification, all areas can be divided into the following classes:

1. forested primary land
2. non-forested primary land
3. potentially forested secondary land
4. potentially non-forested secondary land
5. managed pasture
6. rangeland
7. urban land
8. C3 annual crops
9. C3 perennial crops
10. C4 annual crops
11. C4 perennial crops
12. C3 nitrogen-fixing crops
13. open water

It is not sufficient to simply remap the LUH2 data onto the grid of the INM-CM atmosphere model. The components of the INM RAS Earth system model, including the ocean model, the heat and moisture transfer module, are configured with the fixed land-ocean mask and the original land cover classification. Adapting them for use with any new distributions is a disproportionately difficult task at this stage. Another approach is to

2024, **25** (3), 315–325. doi 10.26089/NumMet.v25r324

Figure 3. Scheme of sequential mapping of land cover types from LUH2 to INM-CM classification

adjust the LUH2 data. For this purpose, the dataset is fitted to the INM-CM land-ocean mask and converted according to the original set of PFTs. The correspondence of all land cover types from both the original INM-CM and LUH2 classifications to four aggregated classes is determined according to Tab. 2. This is done by comparing the spatial distribution of all these types. The aggregated data from the LUH2 project for each year are recalculated for each model cell in accordance with ratio of types from the original INM-CM map.

The sequential mapping of land cover types from the LUH2 classification to the INM-CM one is illustrated in Fig. 3. The land type areas of the intermediate set $\left\{\mathrm{VEG}^j_{\mathrm{Agr}}\right\}_{j=1}^{N_{\mathrm{Agr}}}$ are obtained by aggregating the areas of the types used in the LUH2 project $\left\{\mathrm{VEG}^i_{\mathrm{LU}}\right\}_{i=1}^{N_{\mathrm{LU}}}$:

$$\mathrm{VEG}^j_{\mathrm{Agr}} = \sum_{i \in A_j} \mathrm{VEG}^i_{\mathrm{LU}}, \quad j = 1, \ldots, N_{\mathrm{Agr}}. \tag{5}$$

Here A_j is a set of PFTs from the LUH2 classification corresponding to j aggregate type (according to Tab. 2), $N_{\mathrm{LU}} = 13$ and $N_{\mathrm{Agr}} = 4$ are the number of PFTs in the LUH2 and intermediate classifications respectively. Finally, the areas of the INM-CM types $\left\{\mathrm{VEG}^k_{\text{INM-CM}}\right\}_{k=1}^{N_{\text{INM-CM}}}$ are obtained by multiplying the aggregated areas by the specific PFT ratio $R^{\mathrm{Agr}}_{\text{INM-CM}}$:

$$\mathrm{VEG}^k_{\text{INM-CM}} = R^{\mathrm{Agr}}_{\text{INM-CM}_{kj}} \cdot \mathrm{VEG}^j_{\mathrm{Agr}}, \quad k \in B_j, \tag{6}$$

where B_j is a set of PFTs from the INM-CM classification corresponding to j aggregate type (according to Tab. 2), $N_{\text{INM-CM}} = 13$ is the number of PFTs in the INM-CM classification. The ratio $R^{\mathrm{Agr}}_{\text{INM-CM}}$ is calculated

Table 2. Correspondence of land cover types from INM-CM and LUH2 classifications

INM-CM set	**Intermediate set**	**LUH2 set**
tropical forest	forested land	forested primary land
broadleaf-deciduous trees		
mixed forest		
needleleaf-evergreen trees		potentially forested secondary land
needleleaf-deciduous trees		
trees of savanna		
groundcover only	non-forested land	non-forested primary land
broadleaf shrubs with perennial groundcover		
broadleaf shrubs with bare soil		potentially non-forested secondary land
tundra (trees)		
tundra (groundcover)		rangeland
bare soil		urban land
cultivated areas (trees)	cultivated areas	crops (all) and managed pasture
cultivated areas (groundcover)		
open water	open water	open water

2024, **25** (3), 315–325. doi 10.26089/NumMet.v25r324

from the original INM-CM vegetation dataset $\left\{\mathrm{VEG}^k_{\mathrm{orig}}\right\}_{k=1}^{N_{\text{INM-CM}}}$:

$$R^{\mathrm{Agr}}_{\text{INM-CM}_{kj}} = \frac{\mathrm{VEG}^k_{\mathrm{orig}}}{\sum\limits_{p\in B_j} \mathrm{VEG}^p_{\mathrm{orig}}},\ k \in B_j. \tag{7}$$

In Fig. 4 you can see the global area dynamics of land cover types from 1850 to 2100 according to the new land use database for INM-CM (scenario SSP3-7.0 is selected for the future) and the same distribution for the original surface data used in INM RAS Earth system family. The new parameterization shows a noticeable reduction in the area of forests, grassland and bare soil. At the same time, the area of cultivated land has been increasing enormously: from less than 10 million km^2 in 1850 to 25 million km^2 in 2015 and more than 30 million km^2 in 2100. All these changes in the spatial distribution of the classes between 1850 and 2015 are presented in Fig. 5. Furthermore, a comparison with Fig. 1 shows how much the vegetation types dynamics are underestimated by the original map. Note, tundra and shrub areas are changed little over time and are almost the same as in the original version. This is due to the absence of these types explicitly in the LUH2 classification and their identification within non-forested land according to the ratio from the original map used in INM-CM.

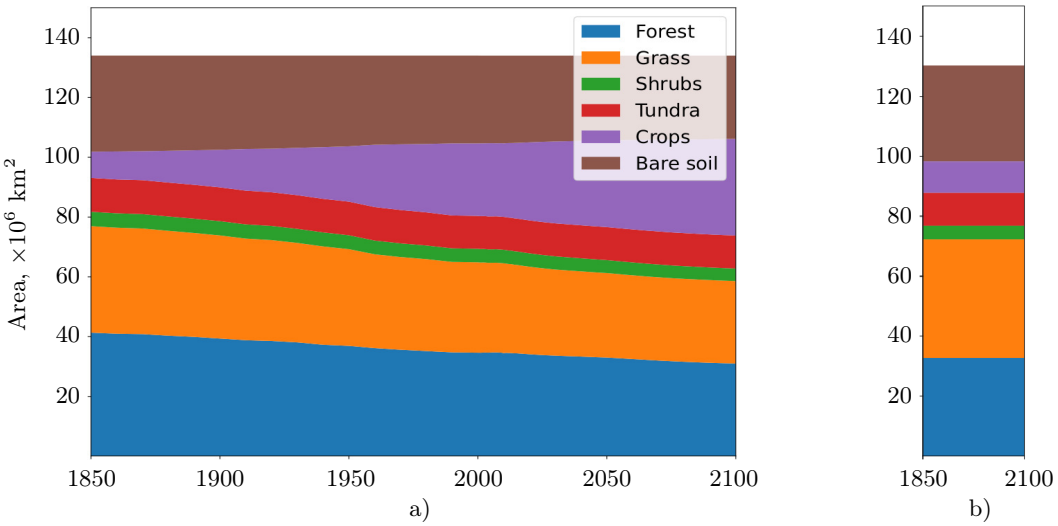

Figure 4. Global land area of different cover types according to
a) the new land use cover database and b) the original INM-CM dataset

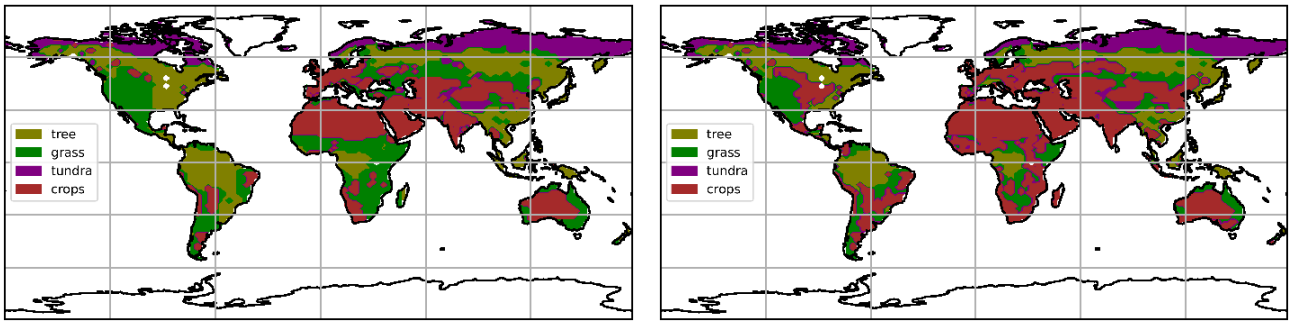

a) 1850 b) 2015

Figure 5. Maps of dominant vegetation types by the new land use database for INM-CM

2.3. New version of INM-CM terrestrial carbon cycle module. The main feature of the modified INM-CM terrestrial carbon cycle module is a more detailed consideration of human impacts on the Earth's ecosystems. Firstly, the effects of land use for vegetation and soil are taken into account according to the new dynamic database of PFTs. Secondly, the effect of harvesting is taken into account. Now, not all of litterfall biomass on cultivated areas goes into the soil pool (C_{SOIL}), but some part of it goes into the fast pool ($C^{\mathrm{fast}}_{\mathrm{SOIL}}$),

2024, **25** (3), 315–325. doi 10.26089/NumMet.v25r324

that is considered as harvesting. The modified equations (1)–(3), considered for each sub-pool corresponding to one of the $N_{\text{veg}} = 13$ PFTs, are given below:

$$\frac{\partial C_{\text{VEG}}}{\partial t} = F_{\text{PSN}} - F_{\text{PLR}} - \frac{C_{\text{VEG}}}{\tau_{\text{VEG}}} - F_{\text{LU}}(t) \cdot C_{\text{VEG}}, \tag{8}$$

$$\frac{\partial C_{\text{SOIL}}}{\partial t} = (1-\alpha) \cdot \frac{C_{\text{VEG}}}{\tau_{\text{VEG}}} - \frac{C_{\text{SOIL}}}{\tau_{\text{SOIL}}} - F_{\text{LU}}(t) \cdot C_{\text{SOIL}}, \tag{9}$$

$$\frac{\partial C^{\text{fast}}_{\text{SOIL}}}{\partial t} = \alpha \cdot \frac{C_{\text{VEG}}}{\tau_{\text{VEG}}} + F_{\text{LU}}(t) \cdot (C_{\text{VEG}} + C_{\text{SOIL}}) - \frac{C^{\text{fast}}_{\text{SOIL}}}{\tau_{\text{fast}}}. \tag{10}$$

Here $F_{\text{LU}}(t)$ is the rate of change of the PFT area ratio in the model cell due to land use, defined by the equation (11), and dimensionless coefficient $\alpha \in [0, 1]$ is the empirical harvest ratio of litterfall biomass (0.1 for trees and 0.25 for groundcover on cultivated areas and 0.0 for other PFTs). These values for α were found during model fitting.

The value F_{LU} describing the land use effect for the j-th PFT ($j = 1, \ldots, N_{\text{veg}}$) is given by the following relationship:

$$F_{\text{LU}_j}(t + \Delta t) = \frac{S_j(t + \Delta t) - S_j(t)}{S_j(t)} \cdot \frac{1}{\Delta t}. \tag{11}$$

Here $S_j(t)$ is the area of the j-th land cover type in the model cell at time t, $\Delta t = 1$ year is the time step of the land use database. The current version of the module assumes that PFT areas $\{S_j(t)\}_{j=1}^{N_{\text{veg}}}$ are updated at the beginning of the year and that the effect of land use change F_{LU} is spread evenly throughout the year. The fluxes F_{PSN} and F_{PLR} are also normalised to the current PFT areas.

3. Numerical experiments. Numerical experiments are carried out with the original [10] and modified versions of the INM-CM terrestrial carbon cycle module. The experiments are performed from 1850 to 2100, including both the historical period (1850–2014) [5] and the future scenario SSP3-7.0 (2015–2100) [14]. The simulations are run with the stand-alone C-cycle module and within the coupled model INMCM6.

The physics of the stand-alone module is fully consistent with the terrestrial carbon cycle in the coupled model. As input data, it uses atmospheric forcings obtained from the INMCM6 output (temperature and humidity at 2 m, incoming shortwave radiation flux, soil temperature and humidity). Moreover, both models use similar prescribed atmospheric CO_2 concentrations and land use data as forcings. Note that in the stand-alone model the time step is increased to one month, because the accumulation and decomposition of terrestrial carbon pools takes at least several months, while the time step in the coupled model is limited by faster heat and moisture transfer processes.

3.1. Initial conditions. To compute historical and scenario experiments with the C-cycle module, it is necessary to set the initial conditions for the carbon pools for the year 1850. For this purpose, we propose to use the steady states generated by the model, corresponding to the end of the pre-industrial period. The achievement of steady states for simulated carbon pools is shown in Fig. 6.

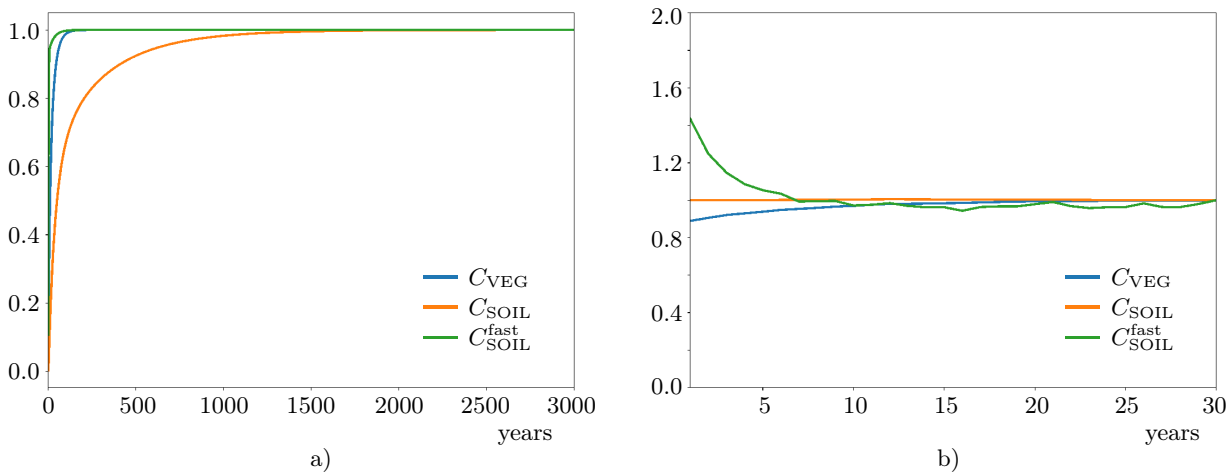

Figure 6. Carbon pools reaching steady states under constant forcings of 1850 (normalised to the final states): a) for stand-alone terrestrial C-cycle module and b) for coupled model INMCM6

2024, **25** (3), 315–325. doi 10.26089/NumMet.v25r324

For the stand-alone model, we perform a spin up run from zero initial pools for 3000 years with all forcings corresponding to 1850. In this case, the final state of the carbon pools is steady (Fig. 6 a) and suitable for the initial state for historical simulations since 1850. Note that the spin up duration is limited by the slow dynamics of the soil pool (C_{SOIL}). This is due to the long characteristic turnover time (τ_{SOIL}), especially in the tundra (see Tab. 1), where the soil carbon pool is maximal.

For the coupled model spin up, the piControl run [5], where all forcings correspond to 1850, is usually used. To obtain steady states of carbon pools for INMCM6, we perform a piControl run using as initial conditions the final state of the pools after the stand-alone C-cycle module spin up. The final state of the coupled model is used as a consistent initial state for it in historical simulations since 1850. One can see from Fig. 6 b that 30 years run with the coupled model is enough. In this case, the limiting factor is the dynamics of the vegetation (C_{VEG}) and rapidly degradable soil ($C^{\mathrm{fast}}_{\mathrm{SOIL}}$) pools, the characteristic turnover times (τ_{VEG} and τ_{fast}, respectively) of which is less or comparable to the soil pool one (Tab. 1). In contrast to the slow soil dynamics, pools with fast dynamics are more sensitive to changes in the near-surface atmosphere associated with the model transition to a steady climate.

Note the computational efficiency of the described technology for the initial state preparation. All calculations are performed on the HPC system of the Marchuk Institute of Numerical Mathematics of the Russian Academy of Sciences. The stand-alone carbon cycle module requires one computational core and simulates about 4500 years per hour. Calculations with the coupled model INMCM6 are carried out in a configuration with 160 computational cores (56 cores per atmosphere model, 56 cores per aerosol block and 48 cores per ocean model) [15]. In this configuration, it simulates approximately 26 years per day. Taking into account the described time scales, the ability to reduce the spin up time for the coupled model by a factor of 100 using the stand-alone version is significant.

4. Results. Figures 7, 8 present the simulated carbon storage in plants and soil by INMCM6 with the new terrestrial carbon cycle module for 2015, and its difference from the original model [8, 10]. First of all, the updated version shows the decrease in stored plant and soil carbon associated with the clarified accounting of

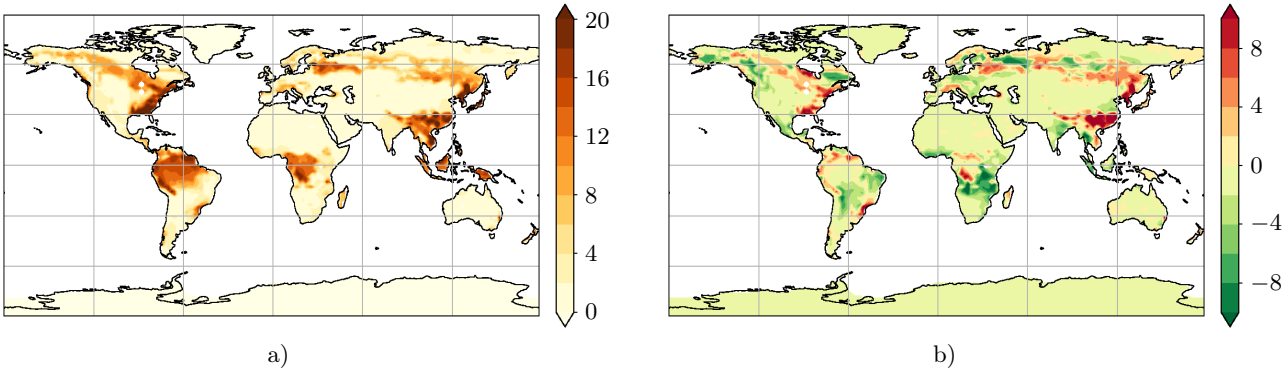

Figure 7. Simulated vegetation carbon [kg/m^2] in 2015 by INMCM6
with a) the new terrestrial carbon cycle module and b) its difference with the old one

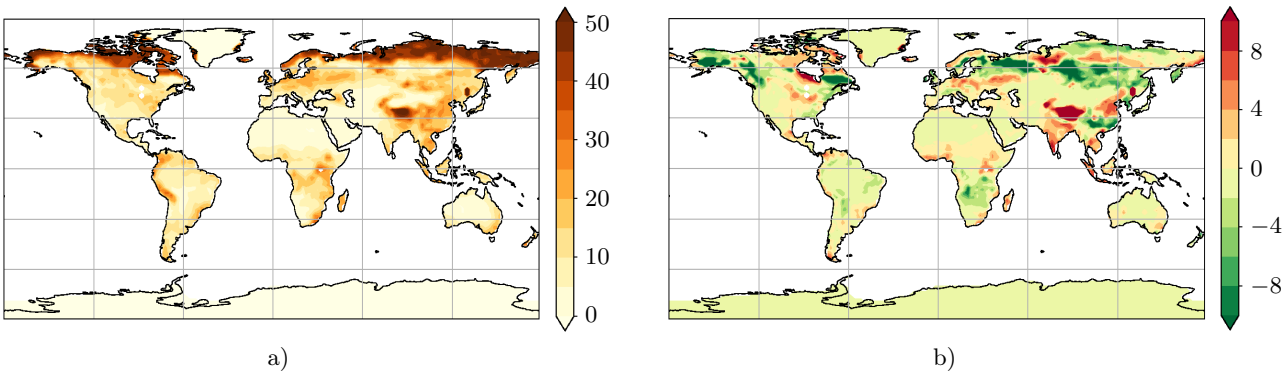

Figure 8. Simulated soil carbon [kg/m^2] in 2015 by INMCM6
with a) the new terrestrial carbon cycle module and b) its difference with the old one

2024, **25** (3), 315–325. doi 10.26089/NumMet.v25r324

deforestation. This is most noticeable for tropical forests, particularly in Brazil and southern Africa. On the other hand, in the mid-latitudes of Eurasia and North America, the new database gives significantly more area for forest instead of grassland than the original one. As a result, the simulated vegetation carbon pool in these areas is higher in case of the new version of the module. At the same time, the soil carbon pool is lower, which is explained by the higher intensity of soil respiration for forest compared to grass.

Figure 9 presents the change in global land carbon storage compared to 1850 simulated by the different versions of the terrestrial carbon cycle module, both in stand-alone mode and within the coupled model INMCM6. This plot is similar to Figure 5.23b from the 6th Assessment Report of the IPCC [1] and shows the difference in carbon stocks compared to the end of the pre-industrial period. The modified version of the module demonstrates good agreement with observational data (Global Carbon Project estimate [2]) in both modes and fits into the CMIP6 multi-model ensemble spread for the historical period (1850–2014) [1, 7]. The key point is that the new parameterization simulates the negative minimum in the second half of the 20th century, which is largely associated with extensive deforestation. For the future scenario SSP3-7.0 (2015–2100), the projection of land carbon stock changes by INMCM6 with the updated carbon module is consistent with the results of other models (about +200 Gt C by 2100 relative to 1850) [1].

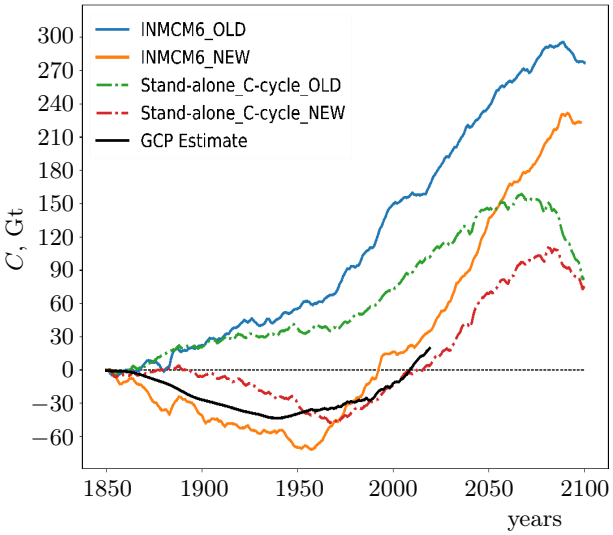

Figure 9. Land carbon storage change simulated by different versions of the INM-CM terrestrial carbon cycle module for the period 1850–2100, compared to observation-based estimates from the global carbon project (GCP) (scenario SSP3-7.0 for the future)

5. Conclusions. In this paper, we present the new terrestrial carbon cycle module for the INM RAS Earth system model family. Its main difference from the previous one is up-to-date description of land use and its changes. The modified version also includes large-scale deforestation in the 20th century and shows its influence on the carbon cycle. In addition, the impact of agriculture on the terrestrial carbon cycle is adjusted through harvest accounting. These modifications to the carbon module are tested in stand-alone mode and also implemented in the coupled model INMCM6. The updates significantly improve the model estimate of the global carbon stock change during the 20th century. In addition, the projections of land carbon uptake during the 21st century from the modified version of INMCM6 are in better agreement with the data from the CMIP6 multi-model ensemble. Further updates of the land C-cycle module may include the effects of fires, as well as carbon cycle in wetlands.

References

1. V. P. Masson-Delmotte, A. Zhai, S. L. Pirani, et al., *Climate Change 2021: The Physical Science Basis* (Cambridge Univ. Press, Cambridge, 2021). doi 10.1017/9781009157896.
2. P. Friedlingstein, M. O'Sullivan, M. W. Jones, et al., "Global Carbon Budget 2023," Earth Syst. Sci. Data, **15** (12), 5301–5369 (2023). doi 10.5194/essd-15-5301-2023.
3. P. J. Lawrence, J. J. Feddema, G. B. Bonan, et al., "Simulating the Biogeochemical and Biogeophysical Impacts of Transient Land Cover Change and Wood Harvest in the Community Climate System Model (CCSM4) from 1850 to 2100," J. Clim. **25** (9), 3071–3095 (2012). doi 10.1175/JCLI-D-11-00256.1.
4. D. M. Lawrence, G. C. Hurtt, A. Arneth, et al., "The Land Use Model Intercomparison Project (LUMIP) Contribution to CMIP6: Rationale and Experimental Design," Geosci. Model Dev. **9** (9), 2973–2998 (2016). doi 10.5194/gmd-9-2973-2016.
5. V. Eyring, S. Bony, G. A. Meehl, et al., "Overview of the Coupled Model Intercomparison Project Phase 6 (CMIP6) Experimental Design and Organization," Geosci. Model Dev. **9** (5), 1937–1958 (2016). doi 10.5194/gmd-9-1937-2016.

2024, **25** (3), 315–325. doi 10.26089/NumMet.v25r324

6. G. C. Hurtt, L. Chini, R. Sahajpal, et al., "Harmonization of Global Land Use Change and Management for the Period 850–2100 (LUH2) for CMIP6," Geosci. Model Dev. **13** (11) 5425–5464 (2020). doi 10.5194/gmd-13-5425-2020.
7. S. K. Liddicoat, A. J. Wiltshire, C. D. Jones, et al., "Compatible Fossil Fuel CO_2 Emissions in the CMIP6 Earth System Models' Historical and Shared Socioeconomic Pathway Experiments of the Twenty-First Century," J. Clim. **34** (8), 2853–2875 (2021). doi 10.1175/JCLI-D-19-0991.1.
8. E. M. Volodin, "Simulation of Present-Day Climate with the INMCM60 Model," Izv. Atmos. Ocean. Phys. **59** (1), 16–22 (2023). doi 10.1134/s0001433823010139.
9. E. Volodin and V. Lykossov, "Parameterization of Heat and Moisture Transfer in the Soil-Vegetation System for Use in Atmospheric General Circulation Models: 1. Formulation and Simulations Based on Local Observational Data," Izv. Atmos. Ocean. Phys. **34** (4), 405–416 (1998).
10. E. M. Volodin, "Atmosphere-Ocean General Circulation Model with the Carbon Cycle," Izv. Atmos. Ocean. Phys. **43** (3), 266–280 (2007). doi 10.1134/s0001433807030024.
11. G. B. Bonan, "Land-Atmosphere Interactions for Climate System Models: Coupling Biophysical, Biogeochemical, and Ecosystem Dynamical Processes," Remote Sens. Environ. **51** (1), 57–73 (1995). doi 10.1016/0034-4257(94)00065-U.
12. J. L. Dorman and P. J. Sellers, "A Global Climatology of Albedo, Roughness Length and Stomatal Resistance for Atmospheric General Circulation Models as Represented by the Simple Biosphere Model (SiB)," J. Appl. Meteorol. Climatol. **28** (9), 833–855 (1989). doi 10.1175/1520-0450(1989)028<0833:AGCOAR>2.0.CO;2.
13. M. F. Wilson and A. Henderson-Sellers, "A Global Archive of Land Cover and Soils Data for Use in General Circulation Climate Models," J. Climatol. **5** (2), 119–143 (1985). doi 10.1002/joc.3370050202.
14. B. C. O'Neill, C. Tebaldi, D. P. van Vuuren, et al., "The Scenario Model Intercomparison Project (ScenarioMIP) for CMIP6," Geosci. Model Dev. **9** (9), 3461–3482 (2016). doi 10.5194/gmd-9-3461-2016.
15. M. Tarasevich, A. Sakhno, D. Blagodatskikh, et al., "Scalability of the INM RAS Earth System Model," in *Lecture Notes in Computer Science* (Springer, Cham, 2024), Vol. 14388, pp. 202–216. doi 10.1007/978-3-031-49432-1_16.

Received
Jule 23, 2024

Accepted for publication
August 26, 2024

Information about the authors

Alexey Yu. Chernenkov — Junior Scientific Researcher; 1) Marchuk Institute of Numerical Mathematics RAS, Gubkina ulitsa, 8, 119333, Moscow, Russia; 2) Institute of Geography RAS, Staromonetniy lane, 29, 119017, Moscow, Russia; 3) Moscow Institute of Physics and Technology (National Research University), Institutskiy pereulok, 9, 141701, Dolgoprudny, Russia.

Evgeny M. Volodin — Dr. Sci., Leading Scientist; 1) Marchuk Institute of Numerical Mathematics RAS, Gubkina ulitsa, 8, 119333, Moscow, Russia; 2) Institute of Geography RAS, Staromonetniy lane, 29, 119017, Moscow, Russia.